Polym. Korea, Vol. 47, No. 2, pp. 171-180 (2023)
https://doi.org/10.7317/pk.2023.47.2.171

ISSN 0379-153X(Print)
ISSN 2234-8077(Online)

포도당 탈수소효소와 합성된 폴리루테늄 매개체를 이용한 전기화학적 포도당 감지

박수빈[#] · 전원용[*,#] · 최영봉[†]

단국대학교 화학과

*성균관대학교 화학공학과, 트랜스레이셔널 나노바이오사이언스 연구센터, 성균바이오융합과학기술원

(2022년 11월 10일 접수, 2023년 1월 16일 수정, 2023년 1월 31일 채택)

Electrochemical Glucose Sensing by Using Glucose Dehydrogenase Enzyme and the Synthesized Poly-ruthenium Mediator

Su-Bin Park[#], Won-Yong Jeon[*,#], and Young-Bong Choi[†]

Department of Chemistry, College of Science & Technology, Dankook University, Dandae-ro, Cheonan-si, Chungnam 31116, Korea
**School of Chemical Engineering, Translational Nanobioscience Research Center, and Biomedical Institute for Convergence at SKKU (BICS), Sungkyunkwan University, Suwon 16419, Korea*

(Received November 10, 2022; Revised January 16, 2023; Accepted January 31, 2023)

초록: 당뇨병의 정확한 진단을 위해 산업체에서는 2세대 포도당센서를 사용해왔다. 2세대 포도당센서의 전자전달 매개체는 철, 루테늄 및 오스뮴과 같은 VIII족 금속으로 이루어져 있으며 본 논문에서는 포도당 탈수소 효소(GDH) 와 감응하는 새로운 전자전달 매개체를 합성하였다. 전기화학적 포도당 센서용 polyvinylimidazole(PVI)-[루테늄(4,4′-diamino-2,2′-bipyridine)$_2$Cl](PVI-[Ru(dam-bpy)$_2$Cl]) 전자전달 매개체의 구조는 ^{1}H nuclear magnetic resonance, Fourier-transform infrared 및 ultraviolet-visible spectroscopy로 측정하였다. 또한, cyclic voltammetry와 multi-potential step을 사용하여 전기화학적 특성을 분석하였다. PVI-[Ru(dam-bpy)$_2$Cl]은 GDH를 사용하여 전극을 제작하였고, 마지막으로, 광범위한 포도당 농도(1-40 mM)에서 전기화학적 선형성이 입증되었다. PVI-[Ru(dam-bpy)$_2$Cl] 전자전달 매개체가 2세대 포도당 바이오센서로서 산업계에서 직접 사용될 수 있을 것으로 기대한다.

Abstract: Diabetes necessitates the use of reliable glucose sensors capable of preventing the onset of complications via accurate and timely diagnosis. Among such sensors is a second-generation glucose amperometric sensor that uses an electrochemical method and is based on a mediator that transfers electrons from the enzyme to the electrode. Group VIII metals, such as iron, ruthenium, and osmium, have conventionally been used, and are synthesized with both electron-withdrawing and -donating ligands. Among these mediators, hexaaminеruthenium(III) transferred electrons generated by glucose via glucose oxidase (GOx) to the electrode, allowing glucose quantification. However, a measurement error of the GOx enzyme was recently discovered due to external oxygen interference; therefore, it is being replaced with the enzyme glucose dehydrogenase (GDH). Hexaaminеruthenium(III) exhibited a low electron transfer efficiency due to electrons stolen during the reaction with the GDH enzyme. Thus, to solve this problem, herein we synthesized a polymer-based ruthenium mediator complex, viz. polyvinylimidazole-[ruthenium(4,4′-diamino-2,2′-bipyridine)$_2$chloride] (PVI-[Ru(dam-bpy)$_2$Cl]) for electrochemical glucose sensing. The structure of the new mediator was determined using ^{1}H nuclear magnetic resonance, Fourier-transform infrared, and ultraviolet-visible spectroscopies. Furthermore, electrochemical properties were determined using cyclic voltammetry and a multi-potential step. PVI-[Ru(dam-bpy)$_2$Cl] interacted favorably with GDH. Finally, electrochemical linearity was demonstrated with a wide range of glucose concentrations (1-40 mM). We anticipate that PVI-[Ru(dam-bpy)$_2$Cl] can be used directly in the industry as a second-generation glucose biosensor.

Keywords: glucose sensor, polymer mediator, glucose dehydrogenase, second generation, electrochemistry.

Introduction

For various reasons, including diet and lifestyle, diabetes has emerged as a major health problem worldwide. Diabetes is associated with a high mortality rate and various complica-

[#]S.-B. Park and W.-Y. Jeon contributed equally to this paper as the first authors.
[†]To whom correspondence should be addressed.
chem0404@dankook.ac.kr, ORCID 0000-0002-3862-456X

tions. Therefore, accurate and appropriate diabetes diagnosis and treatment require reliable blood sugar monitoring. Many researchers are still working on developing a blood glucose sensor that can monitor glucose in a reliable, accurate, low-cost, and quick manner.[1-3] Optical, calorimetric, and electrochemical methods are commonly used to develop glucose biosensors. Among them is the use of an electrochemistry-based glucose biosensor, and in particular, an amperometric enzyme glucose sensor, which aids the diagnosis and treatment of diabetes.[1,4-6] Initially, researchers studied first- and second-generation glucose sensors based on the glucose oxidase (GOD) enzyme. Among them is a second-generation sensor that uses mediators (artificial electron acceptors), such as metal complexes, to achieve rapid redox reactions while avoiding interference from other redox species. This is because the first-generation sensor, which uses blood oxygen as an electron transfer medium, has an error between regions, genders, and people, making it ineligible for launch.[1,5,6] Group VIII transition metal complexes such as iron, ruthenium, osmium, ferricyanide, hexaammineruthenium(III), or organic substances like quinone are commonly used as mediators. Hexaammineruthenium(III), which has a high solubility in water and excellent sensitivity to GOD enzyme, has been commercialized because of its low redox potential, which does not overlap with those of other interfering substances.[7,8] The GOD enzyme which has a high selectivity for D-glucose (substrate), has been used in glucose sensors and diagnostic kits. However, because the GOD enzyme uses oxygen as an electron acceptor, it is greatly affected by the dissolved oxygen concentration in the blood.[9-12] Recently, a glucose dehydrogenase (GDH) enzyme, which does not require an oxygen cofactor, has been used to solve this problem. The GDH enzyme, like GOD, can selectively oxidize glucose, but the electron acceptor is unaffected by oxygen; therefore, the error for oxygen in the blood is relatively small.[1,9,13] GDH contains various cofactors, including pyrroloquinoline (PQQ), nicotine adenine dinucleotide (NAD), and flavin adenine dinucleotide (FAD). PQQ-GDH, NAD-GDH, and FAD-GDH have high glucose selectivity. However, PQQ-GDH exhibits high selectivity for substrates like glucose, lactose, cellobiose, and maltose. In the case of NAD-GDH, the NAD cofactor is oxidized, necessitating the use of an additional catalyst. Although FAD-GDH exhibits slightly lower activity than PQQ-GDH and NAD-GDH, it has excellent selectivity for glucose and shows thermal stability. It also does not require an additional catalyst. Because of these advantages, many researchers are investigating the enzymatic glucose sensor based on the FAD-GDH enzyme.[13]

However, the FAD-GDH enzyme exhibits poor electron transfer with the hexaammineruthenium (III) mediator.[7,8] This is because oxygen dissolved in the blood promotes oxidation of hexaammineruthenium (III) when the FAD-GDH enzyme transfers the electron to hexaammineruthenium (III) of low formal potential at the electrode. In other words, the FAD-GDH enzyme on the electrode selectively oxidizes glucose in the blood, and the electrons generated are supplied to hexaammineruthenium (III). The resultant reduced hexaammineruthenium (II) provides electrons to the electrode before returning to the oxidized hexaammineruthenium (III) form to measure the glucose level. However, the electrons of glucose are stolen as the reduced hexaammineruthenium (II) provides electrons to oxygen in the blood and oxidizes to form the oxidized hexaammineruthenium (III). Therefore, there is a fatal disadvantage that the level of glucose is underestimated, resulting in a low-concentration signal.[14]

To develop a useful GDH-based glucose sensor, it is necessary to develop a ruthenium–osmium complex mediator that can efficiently transfer electrons to the electrode by reacting with the FAD-GDH enzyme. Complexes in the form of monomers using a bipyridine-based ligand, which can easily coordinate with ruthenium and osmium metals, have been studied.[15-18] However, monomer-type mediators have a problem; the modification method with enzyme and electrode surface is difficult, and they are easily degassed into the solution phase when glucose is measured, resulting in inefficient electron transfer on the electrode surface. Thus, the development of a metal mediator using a polymer has sparked significant interest.[19,20]

In this study, a polymer-based ruthenium complex mediator that responds to FAD-GDH was synthesized and its electrochemical properties for glucose sensing were investigated. To synthesize a low-potential ruthenium complex, hydrophilic poly(vinyl imidazole) (PVI) was used to improve solubility in water and adsorption at the electrode and a 4,4′-diamino-2,2′-bipyridine (dam-bpy) ligand donating electron was coordinated.[21] Nuclear magnetic resonance spectroscopy (NMR), ultraviolet-visible spectroscopy (UV-vis), and Fourier-transform infrared (FTIR) spectroscopies were used to confirm the chemical structure of the synthesized complexes, and the zeta potential was measured to analyze the cation and dispersion of the complexes. We measured its electrochemical performance using the potentiostat techniques of cyclic voltammetry (CV) and multi-potential step (MPS). Finally, a wide range of glucose concentrations from 1 to 40 mM were tested in the presence of interfering species, such as ascorbic acid (AA), dopamine

(DA), and uric acid (UA). Therefore, we anticipate that our new polymer-based mediator can be used a glucose sensor based on the GDH enzyme.

Experimental

Reagents and Materials. Ruthenium (III) chloride hydrate, 4,4′-diamino-2,2′-bipyridine (dam-bpy), and GDH (FAD-dependent GDH-584 U/mg) were purchased from Alfa Aesar Co. (Ward Hill, MA, USA), Carbosynth Ltd. (Compton, UK), and Toyobo Co. (Japan), respectively. 1-Vinylimidazole, poly(ethylene glycol) diglycidyl ether (PEGDEG), D-(+)-glucose, and 2,2′-azobis(2-methylpropionitrile) (AIBN) were purchased from Sigma-Aldrich Co. (Milwaukee, WI, USA). Phosphate buffered saline (1 X PBS,), sodium dihydrogen phosphate (NaH_2PO_4, 4.3 mM), sodium hydrogen phosphate (Na_2HPO_4, 15.1 mM), sodium chloride (NaCl, 140 mM), and all other solutions were prepared using deionized (DI) Milli-Q water (Millipore, Japan). Analytical reagents were used without further purification.

Synthesis of [Ru(dam-bpy)$_2$Cl$_2$]. [Ru(dam-bpy)$_2$Cl$_2$] was synthesized by modifying a previously demonstrated method.[15,17,18] $RuCl_3 \cdot xH_2O$ (37.7 mg, 0.1817 mM) and dam-bpy (67.7 mg, 0.3634 mM) were heated to reflux for 30 min in anhydrous ethylene glycol (10 mL). The crude product was isolated after cooling to room temperature by dropwise addition of the reaction mixture into a mixture of acetone (50 mL) and diethyl ether (200 mL). The precipitate was then dissolved in 50 mL of ethanol before being purified via column chromatography on aluminum oxide with ethanol as a developing solvent. This concentrated solution was re-precipitated by adding it dropwise to 200 mL of diethyl ether. Finally, it was filtered under reduced pressure with a 0.45 μm membrane filter, and the powder was dried for one day in a vacuum oven at 60 ℃.

Synthesis of PVI. PVI was synthesized as previously demonstrated.[22,23] For 48 h at 70 ℃, 1-Vinylimidazole (1.92 mL, 21.2 mM) was dissolved with AIBN (18.5 mg, 0.11 mM) as a starting agent in 100 mL of benzene solvent. The polymer was then dissolved in 30 mL methanol and precipitated in 500 mL of diethyl ether. The precipitated polymer was filtered under reduced pressure and dried in a vacuum oven at 40 ℃.

Synthesis of PVI-[Ru(dam-bpy)$_2$Cl]. [Ru(dam-bpy)$_2$Cl$_2$] (42.4 mg) and PVI (42.4 mg) were reacted in 15 mL of ethylene glycol and refluxed at 160 ℃ for 3 h (Scheme 1). Following cooling to room temperature, it was added dropwise to 400 mL of diethyl ether to separate the product from the solvent. After dissolving the precipitate in 50 mL of DI water, the solution was filtered and concentrated using ultrafiltration discs. The concentrated solution was re-precipitated with 500 mL of diethyl ether before drying in a vacuum oven at 40 ℃.[17,24] The GPC results of PVI and PVI-[Ru(dam-bpy)$_2$Cl] were summarized in Table 1.

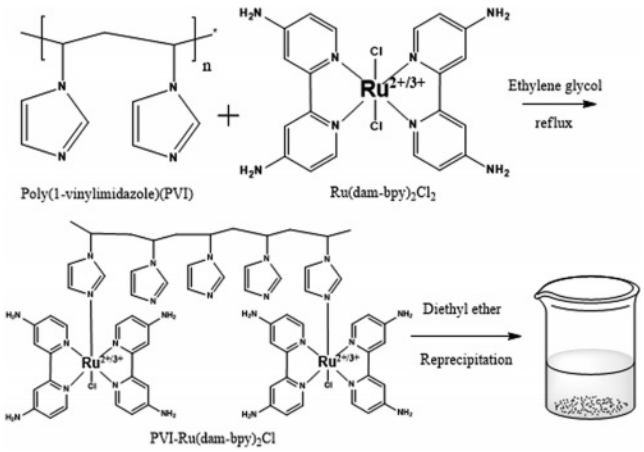

Scheme 1. Synthesis scheme for PVI-[Ru(dam-bpy)$_2$Cl] mediator.

Table 1. GPC Results of PVI and PVI-[Ru(dam-bpy)$_2$Cl]$^{+/2+}$

(g/mol)	PVI	PVI-[Ru(dam-bpy)$_2$Cl]
M_n	13,197	30,088
M_w	27,168	44,134
M_z	45,290	61,962
M_p	25,509	35,644

Characterization of [Ru(dam-bpy)$_2$Cl$_2$] and PVI-[Ru(dam-bpy)$_2$Cl]. The chemical structures of successfully synthesized [Ru(dam)-bpy)$_2$Cl$_2$] and PVI-[Ru(dam-bpy)$_2$Cl] were examined using ^{1}H NMR (Varian Ascend 500, 500 MHz), UV-vis spectroscopy (Model 8453, Agilent Technologies, Shanghai, China) and FTIR (Model Cary 630, Agilent Technologies, Shanghai, China). Using zeta potential, the cationicity and dispersibility of PVI-[Ru(dam-bpy)$_2$Cl] mediator particles were confirmed (SZ-100, Horiba, Hiroshima, Fuchu, Japan).

Electrochemical Measurements. The CHI 660B software was used to measure all electrochemical experiments (CH Instruments, Inc., Austin, TX, USA). The working electrode is a screen-printed carbon electrode (SPCE, with a diameter of 3.5 mm). A platinum wire having a diameter of 0.5 mm, and a micro Ag/AgCl (3.0 M KCl, Cypress, Lawrence, KS, USA) was used as reference and counter electrodes, respectively. To prepare the enzyme electrode for glucose measurement, GDH (40 mg/mL in PBS, 4 μL), [Ru(dam-bpy)$_2$Cl$_2$] or PVI-[Ru(dam-

bpy)$_2$Cl] (10 mg/mL in DI water, 4 μL), and PEGDGE (10 mg/mL in DI water, 1 μL) were adsorbed onto SPCE with a micropipette and dried in a desiccator at 36 ℃ for 12 h. CV measured the electrical reaction of SPCE adsorbed with enzyme and mediator using a 40-μL glucose solution dissolved in 1X PBS. The CV experiment was performed to confirm the response to various glucose concentrations (1.0, 2.5, 5.0, 10.0, 20.0, 30.0, and 40.0 mM) at 0.3 and 0.4 V compared to Ag/AgCl. The GDH enzyme was tested under the same conditions as before to confirm its oxygen effect. The 10 mM glucose solution (in PBS) was purged with air, N_2, and O_2 for 15 min to confirm the CV signals. The MPS was used to test the effect of interfering substances such as AA, DA, and UA (0.1 mM in PBS), which are other electrochemical species in the body, at 0.3 and 0.4 V compared to Ag/AgCl.

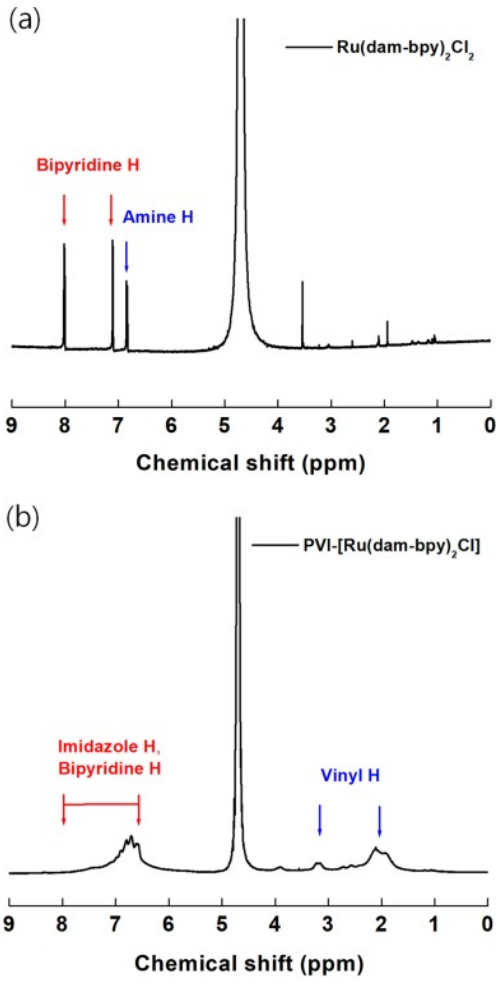

Figure 1. NMR spectra of (a) [Ru(dam-bpy)$_2$Cl$_2$]; (b) PVI-[Ru(dam-bpy)$_2$Cl] mediator.

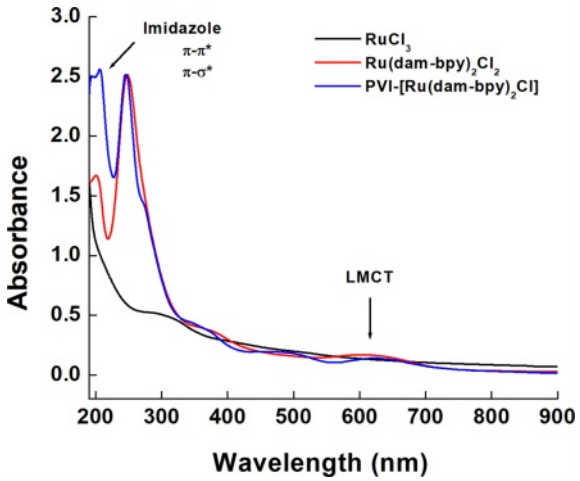

Figure 2. UV-vis spectra of $RuCl_3$ (black line), [Ru(dam-bpy)$_2$Cl$_2$] (red line), and PVI-[Ru(dam-bpy)$_2$Cl] (blue line).

Results and Discussion

Spectroscopic characterization of [Ru(dam-bpy)$_2$Cl$_2$] and PVI-[Ru(dam-bpy)$_2$Cl]. The successful synthesis of [Ru(dam-bpy)$_2$Cl$_2$] and PVI-[Ru(dam-bpy)$_2$Cl] was confirmed by ^{1}H NMR, UV-vis spectrophotometer, and FTIR spectrophotometer. Figure 1 depicts the ^{1}H NMR (D_2O, 500 MHz) result for the amine group (s, ^{4}H, -NH_2) of [Ru(dam-bpy)$_2$Cl$_2$] at 6.84 ppm. We also confirmed C-H bonding at 7.11 ppm (d, ^{2}H, JHH = 4.88 Hz, H5,5') and 8.01 ppm (s, ^{2}H, H3,3') positions 3 and 5 of pyridine, respectively.[25,26] Figure 1(b) shows the vinyl group peaks of PVI-[Ru(dam-bpy)$_2$Cl] at 2.11 and 3.2 ppm. Furthermore, it was confirmed that the result of PVI-[Ru(dam-bpy)$_2$Cl] showed broad peak between 6.7 and 8.0 ppm caused by the polymer's imidazole ring and bipyridine.[27-29] Finally, integrated results showed that ratios of PVI and PVI-[Ru(dam-bpy)$_2$Cl] were 9.2 : 1.

Figure 2 shows the UV-vis spectrophotometer readings after dissolving $RuCl_3$, [Ru(dam-bpy)$_2$Cl$_2$] and PVI-[Ru(dam-bpy)$_2$Cl] in DI water (0.5 mg/mL). The spectrum of [Ru(dam-bpy)$_2$Cl$_2$] revealed an absorption signal at 603 nm, which is in the visible region. A ruthenium (III) monomer ligand-to-metal charge transfer (LMCT) band.[30-32] The tendency of the peak to be red-shifted due to polymer coordination was confirmed in the spectrum of PVI-[Ru(dam-bpy)$_2$Cl]. Also, the π-σ* and π-π* transitions of the imidazole ring of PVI and the π-π* absorption were confirmed by the peaks at 194 and 206 nm, respectively.[33]

The FTIR spectrum of [Ru(dam-bpy)$_2$Cl$_2$] shows an N-H bond at 1600 cm^{-1} and symmetric and asymmetric stretching of

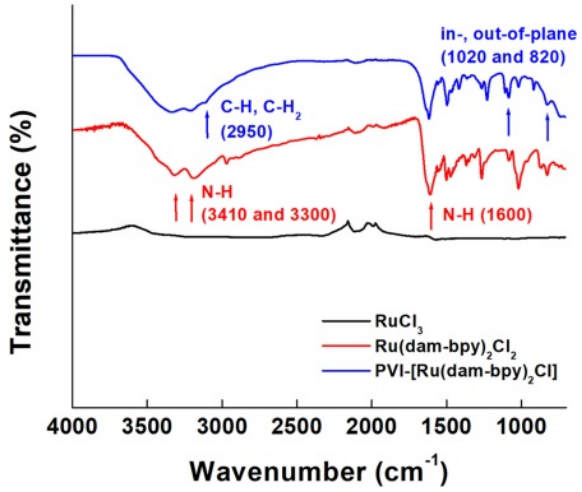

Figure 3. FTIR spectra of $RuCl_3$ (black line), [Ru(dam-bpy)$_2$Cl$_2$] (red line), and PVI-[Ru(dam-bpy)$_2$Cl] (blue line).

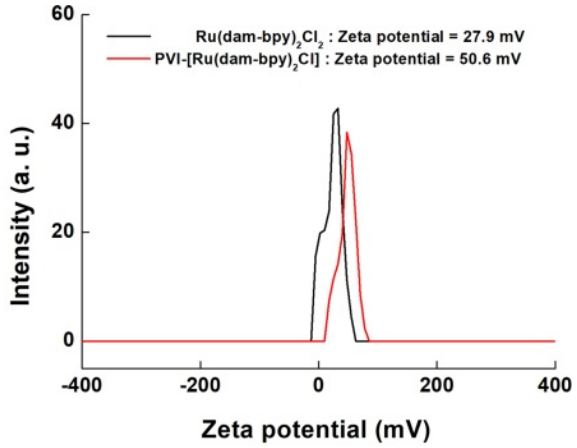

Figure 4. Zeta potential spectra of [Ru(dam-bpy)$_2$Cl$_2$] (black line), and PVI-[Ru(dam-bpy)$_2$Cl] (red line).

N-H at 3410 and 3300 cm^{-1}, respectively (Figure 3).[30,34] The CH and CH_2 stretching peaks of the polymer backbone were weakly confirmed at 2950 cm^{-1} in the spectrum of PVI-[Ru(dam-bpy)$_2$Cl], and the in-plane bending peak was confirmed near 1020 cm^{-1}. Furthermore, the out-of-plane bending peak of the pyridine ring was observed at 820 cm^{-1}, implying the presence of PVI-[Ru(dam-bpy)$_2$Cl].[35,36]

Figure 4 shows the zeta potential result, which confirms the presence of cations and dispersion of the solution. The potentials of [Ru(dam-bpy)$_2$Cl$_2$] and PVI-[Ru(dam-bpy)$_2$Cl] dissolved in DI water were +27.9 and +50.6 mV, respectively. According to the results, the particles exhibited a positive charge in the water solvent. It is well known that a potential of ≥ 30 mV is required for good physical stability, and a potential of ≥ 60 mV is required for excellent physical stability.[37] Therefore, it was confirmed that PVI-[Ru(dam-bpy)$_2$Cl] has a higher zeta potential than [Ru(dam-bpy)$_2$Cl$_2$]. Finally, PVI-[Ru(dam-bpy)$_2$Cl] dispersion stability increased dramatically when coordinated with a hydrogel polymer.

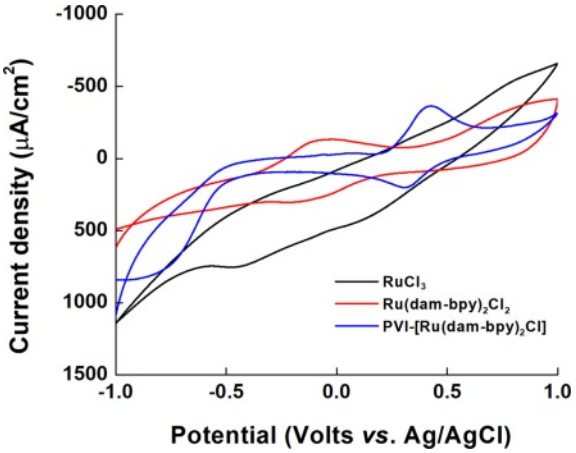

Figure 5. Cyclic voltammograms of $RuCl_3$ (black line), Ru(dam-bpy)$_2$Cl$_2$ (red line), and PVI-[Ru(dam-bpy)$_2$Cl] (blue line).

Electrochemical Characterization of PVI-[Ru(dam-bpy)$_2$Cl]. The electrochemical properties of the synthesized PVI-[Ru(dam-bpy)$_2$Cl] were measured using CV. For the measurement conditions, 10 mg/mL (indicating 10.02 mM concentration) PVI-[Ru(dam-bpy)$_2$Cl] solution, first dissolved in DI water, and then mixed in 1X PBS buffer (1:1, v/v), was used, and CV was measured on a SPCE. The cyclic voltammograms in Figure 5 show the redox peaks of $RuCl_3$ and [Ru(dam-bpy)$_2$Cl$_2$] (E° = -0.1711 V). Furthermore, the E° of PVI-[Ru(dam-bpy)$_2$Cl] showed an oxidation/reduction potential at +0.3675 V with approximately 500-mV shift in the positive potential. The oxidation/reduction potential of [Ru(dam-bpy)$_2$Cl$_2$] is generated at a negative potential by 4,4′-Diamino-2,2′-bipyridine in which NH_2, an electron-donating ligand, is bound to ruthenium. The PVI increased the number of bonds coordinated to ruthenium, and the imidazole group as the electron-withdrawing ligands generated oxidation/reduction potential in PVI-[Ru(dam-bpy)$_2$Cl].

Figure 6 depicts the effect of changing the scan rate (0.01 to 2.00 V/s) on the current signal for confirming the performance of PVI-[Ru(dam-bpy)$_2$Cl] as a mediator and the diffusion effect in the solution phase.[38,39] PVI-[Ru(dam-bpy)$_2$Cl] exhibits quasi-reversible redox peaks at E° = 0.3675 V (Ag/AgCl) in Figure 6. These findings imply that PVI-[Ru(dam-bpy)$_2$Cl] is an appropriate, fast, and reversible redox mediator for electrochemical analysis. Furthermore, the results of the current

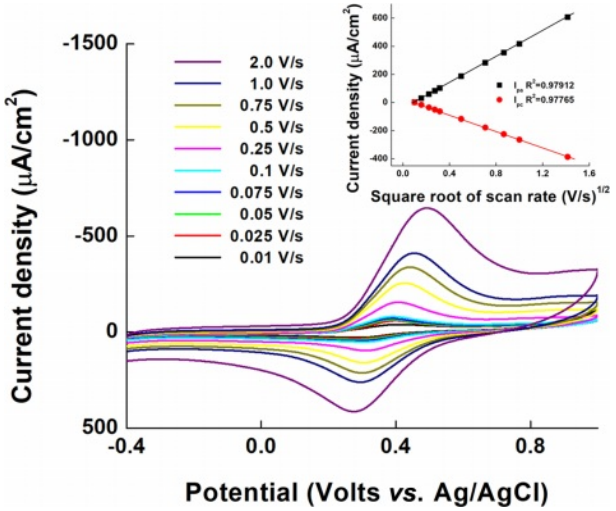

Figure 6. Cyclic voltammograms of PVI-[Ru(dam-bpy)$_2$Cl] at various scan rates from 0.01 to 2.0 V/s.

density according to the square root of the scan rate (inset Figure 6) show the linearity of the PVI-[Ru(dam-bpy)$_2$Cl] anodic (I_{pa}) and cathodic (I_{pc}) peaks with R^2 of 0.979 and 0.978, respectively. This result indicates that the diffusion process effectively controls the electron movement process.

Optimization of pH, GDH Concentration, and O_2 Effect. The CV results of PVI-[Ru(dam-bpy)$_2$Cl] (4.5 mM) for pH optimization in citrate buffer (pH 4), PBS solution (pH 7), and borate buffer (pH 9) are shown in Figure 7(a). The electrode was fabricated by casting a solution of 40 mg/mL FAD-GDH, 10 mg/mL PVI-[Ru(dam-bpy)$_2$Cl] (10.02 mM), and 10 mg/mL PEGDGE (4:4:1, v/v) enzyme. The electrode was then fully dried in the desiccator oven (35 ℃) for 1 d. The maximum potential of PVI-[Ru(dam-bpy)$_2$Cl] at each pH and its anodic peak potential (E_{pa}) and I_{pa} were compared. The tendency to shift to positive potential was confirmed as the pH increased, and the highest current signal was observed in the phosphate buffer saline (pH 7) at the same glucose concentration. This demonstrated that the glucose response was smooth in the pH 7 range, a physiological condition.

Figure 7(b) depicts a bar graph based on CV to optimize the FAD-GDH enzyme at concentrations of 20, 30, 40, 60, and 80 mg/mL in 1X PBS. The electrode was fabricated by casting each enzyme solution of FAD-GDH (20, 30, 40, 60, and 80 mg/mL), 10 mg/mL PVI-[Ru(dam-bpy)$_2$Cl] (10.02 mM), and 10 mg/mL PEGDGE (4:4:1, v/v). The electrode was then fully dried in the desiccator oven (35 ℃) for 1 d. The data was collected from CV results in a 40 mM glucose solution (1X PBS). The current density was calculated using the CV result at 0.3 V.

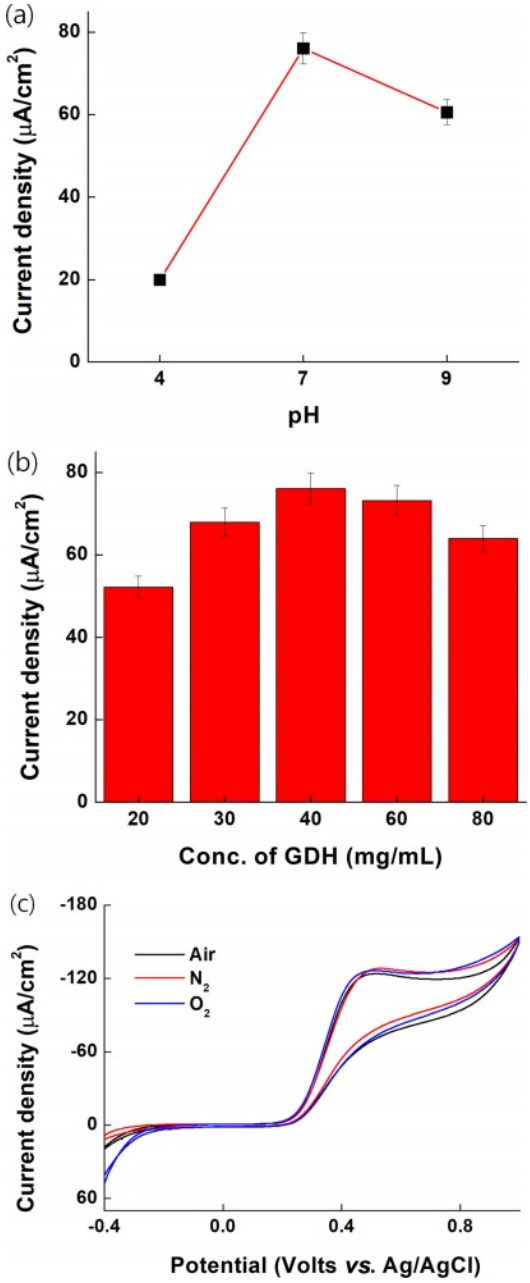

Figure 7. Characterization of current density at different (a) pH; (b) concentration of enzyme; (c) gas (air, nitrogen, and oxygen).

Because of the optimized amount of enzyme, the 40 mg/mL FAD-GDH enzyme concentration indicated the highest current density, after which the current density decreased after that amount. We believe that many enzymes covered the electrode, interfering with electron transfer between the electrode solution and the electrode. Therefore, we selected a FAD-GDH enzyme concentration of 40 mg/mL for our sensor application.

The result shown in Figure 7(c) confirms that the oxygen

concentration in the sample has no effect on FAD-GDH. The CV result was 5 mM glucose purged for 15 min with air, N_2, and O_2 on an electrode fixed with FAD-GDH enzyme (40 mg/mL) and PVI-[Ru(dam-bpy)$_2$Cl] (4.53 mM). Because there was no difference in the current signal values for purging the three gases, it was confirmed that the FAD-GDH enzyme, unlike the GOD enzyme, was not significantly affected by oxygen.

Glucose Sensing. The oxidation catalytic current of various glucose concentrations (1.00 to 40.00 mM in 1XPBS) in SPCE immobilized with GDH enzyme and synthesized PVI-[Ru(dam-bpy)$_2$Cl] was measured.

The performance as a glucose sensor mediator was confirmed with CV and MPS. The oxidation catalyst current of PVI-[Ru(dam-bpy)$_2$Cl] starts at a potential of 0.25 V, as shown in Figure 8(a). The MPS result was measured at 0.3 V for 5 s (inset Figure 8(b)) to test the sensitivity as a glucose sensor. The linearity R^2 was 0.99560, and the relative standard deviation (RSD) was 5.10% after confirming the correlation of the oxidation catalyst current for each concentration (Figure 8(b)). The limit of detection (LOD) and limit of quantification (LOQ) were 0.238872 and 0.716616 mM, respectively. It responds to a wide range of glucose concentrations, from low to high, and the performance of the mediator applicable to the glucose sensor was confirmed.

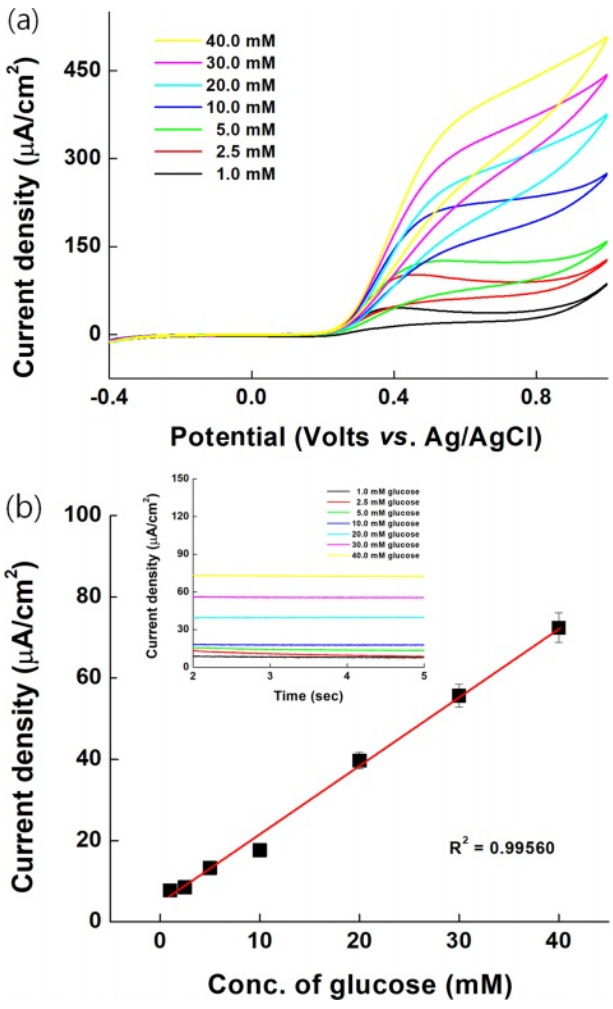

Figure 8. Electrochemical measurements for glucose on PVI-[Ru(dam-bpy)$_2$Cl] based on enzyme electrode: (a) cyclic voltammograms; (b) calibration curve for the anodic current at 0.3 V *vs.* Ag/AgCl.

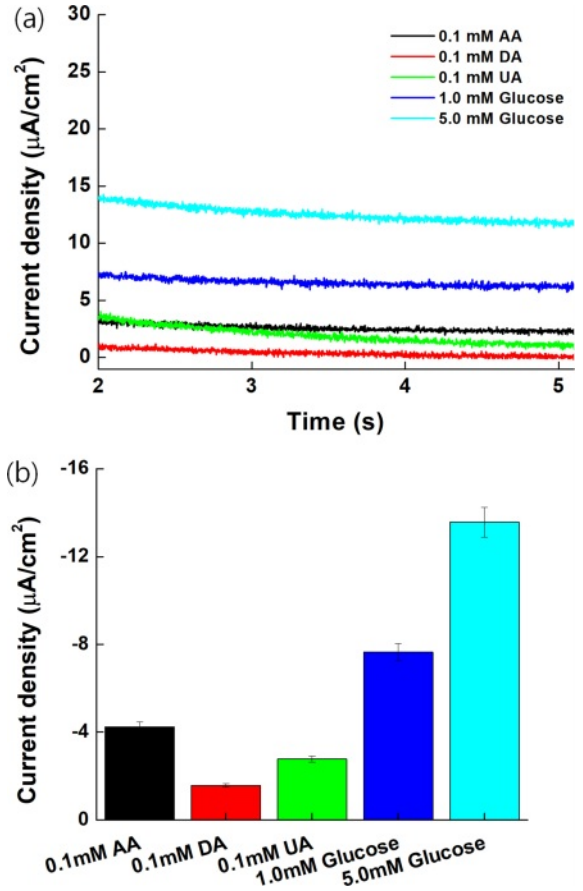

Figure 9. MPS result with glucose (1.0 and 5.0 mM) and various interference species such as 0.1 mM AA, 0.1 mM UA, and 0.1 mM DA.

Interference Effect. Figure 9(a) depicts the MPS results of 1.0 and 5.0 mM glucose, 0.1 mM AA, 0.1 mM DA, and 0.1 mM UA, which are representative electrochemical reaction species to assess the interference effect with PVI-[Ru(dam-bpy)$_2$Cl].[40-42] Interfering substances with high oxidation potential exhibited insignificant oxidation current values and no effect on the oxidation potential of PVI-[Ru(dam-bpy)$_2$Cl]. Figure 9(b) depicts a bar graph to better illustrate the results. When compared to

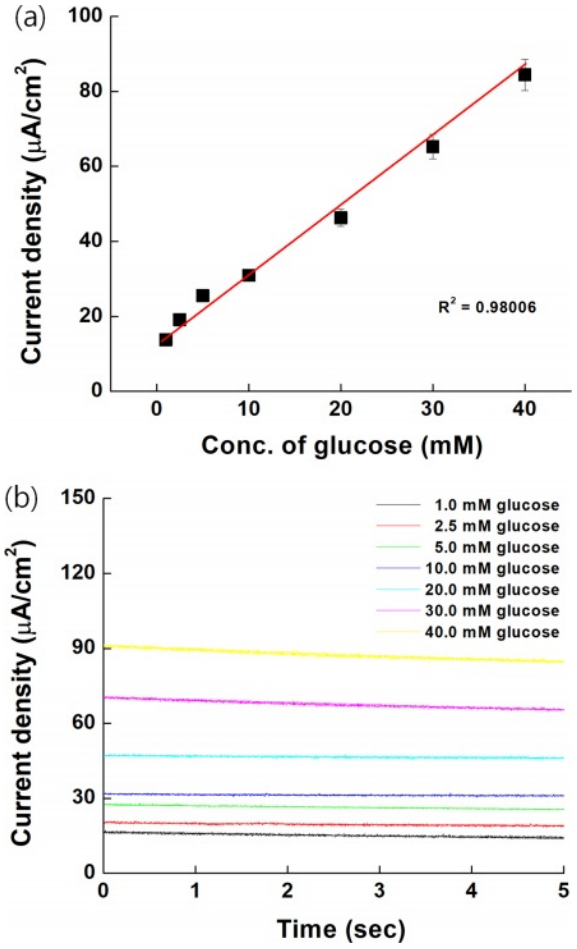

Figure 10. (a) Calibration curve; (b) MPS result on serum samples for the anodic current at 0.3 V *vs*. Ag/AgCl.

1.0 mM glucose, the current density of interfering species displayed a low signal.

Spiking Test on Serum Samples. The spiking test results were carried out on serum sample as shown Figure 10. The current density was slightly increased compared with Figure 8 because of oxidized form on serum. However, the response of our electrodes showed good linearity (R^2=0.98006). This means that our mediator could be used as a GDH-based glucose sensor.

Conclusions

Diabetes causes various complications, including cerebral infarction, arteriosclerosis, and high blood pressure, so it is critical to diagnose and treat blood glucose. Sensors have been developed for this purpose, but most glucose sensors use the GOD enzyme. The GOD enzyme, however, has a disadvantage that an additional oxidation current signal appears as a result of the reaction with oxygen in the blood and air, resulting in an error in the measurement signal value. The FAD-GDH enzyme was used in this study to develop a fast and reliable blood glucose sensor by using a polymer-ruthenium complex with a cationic charge as an electron transport medium and eliminating the error in the measured current signal caused by oxygen. First, using ruthenium chloride and 4,4′-diamino-2,2′-bipyridine, a $[Ru(dam\text{-}bpy)_2Cl_2]^{2+/3+}$ complex was synthesized, and this complex was combined with poly-vinylimidazole to form a PVI-$[Ru(dam\text{-}bpy)_2Cl]^{+/2+}$ complex which was then used as an electron transport mediator. Second, a solution of PVI-$[Ru(dam\text{-}bpy)_2Cl]^{+/2+}$ (10 mg/mL), FAD-GDH enzyme (40 mg/mL), and PEGDEG (10 mg/mL) as a crosslinking agent was casted on the SPCEs electrode in a volume ratio of 4:4:1. The blood glucose sensor based on PVI-$[Ru(dam\text{-}bpy)_2Cl]$/GDH/SPCEs was CV-characterized and demonstrated linearity to glucose in the 1-40 mM range. Furthermore, quantitative analysis of glucose between 1 and 40 mM by MPS confirmed the linearity (R^2 = 0.99560) and RSD (5.10014%) at 0.3 V of potential. The LOD and LOQ values were 0.238872 and 0.716616 mM, respectively, and the synthesized PVI-$[Ru(dam\text{-}bpy)_2Cl]$ demonstrated that it could function well as an electron transfer mediator of the blood glucose sensor in the glucose range of 1-40 mM. Finally, this study explored and validated the FAD-GDH enzyme-based electrochemical glucose sensor electrode as a selective and quantitative glucose sensor for diabetes prevention.

Acknowledgments: The present research was supported by the research fund of Dankook University in 2022.

Conflict of Interest: The authors declare that there is no conflict of interest.

References

1. Heller, A; Feldman, B. Electrochemical Glucose Sensors and Their Applications in Diabetes Management. *Chem. Rev.* **2008**, 108, 2482-2505.
2. Reach, G.; Wilson, G. S. Can Continuous Glucose Monitoring be Used for the Treatment of Diabetes. *Anal. Chem.* **1992**, 64, 381A-386A.
3. Turner, A. P.; Chen, B.; Piletsky, S. A. In Vitro Diagnostics in Diabetes: Meeting the Challenge. *Clin. chem.* **1999**, 45, 1596-1601.
4. Kobos, R. K. Enzyme-based Electrochemical Biosensors. *TrAC Tre. in Anal. Chem*. **1987**, 6, 6-9.
5. Chen, C.; Xie, Q.; Yang, D.; Xiao, H.; Fu, Y.; Tan, Y.; Yao, S. Recent Advances in Electrochemical Glucose Biosensors: a

Review. *RSC Adv.* **2013**, 3, 4473-4491.
6. Wang, J. Glucose Biosensors: 40 Years of Advances and Challenges. *Electroanalysis: An Int. J. Dev. Fund. Prac. Asp. Elect.* **2001**, 13, 983-988.
7. Okurita, M.; Suzuki, N.; Loew, N.; Yoshida, H.; Tsugawa, W.; Mori, K.; Kojima, K.; Klonoff, D. C.; Sode, K. Engineered Fungus Derived FAD-dependent Glucose Dehydrogenase with Acquired Ability to Utilize Hexaammineruthenium (III) as An Electron Acceptor. *Bioelectrochem.* **2018**, 123, 62-69.
8. Loew, N.; Tsugawa, W.; Nagae, D.; Kojima, K.; Sode, K. Mediator Preference of Two Different FAD-dependent Glucose Dehydrogenases Employed in Disposable Enzyme Glucose Sensors. *Sens.* **2017**, 17, 2636.
9. Wang, J. Electrochemical Glucose Biosensors. *Chem. Rev.* **2008**, 108, 814-825.
10. Horaguchi, Y.; Saito, S.; Kojima, K.; Tsugawa, W.; Ferri, S.; Sode, K. Engineering Glucose Oxidase to Minimize the Influence of Oxygen on Sensor Response. *Elect. Act.* **2014**, 126, 158-161.
11. Tang, Z.; Louie, R. F.; Lee, J. H.; Lee, D. M.; Miller, E. E.; Kost, G. J. Oxygen Effects on Glucose Meter Measurements with Glucose Dehydrogenase-and Oxidase-based Test Strips for Point-of-care Testing. *Crit. Care Med.* **2001**, 29, 1062-1070.
12. Okuda-Shimazaki, J.; Yoshida, H.; Sode, K. FAD Dependent Glucose Dehydrogenases-Discovery and Engineering of Representative Glucose Sensing Enzymes. *Bioelectrochem.* **2020**, 132, 107414.
13. Ferri, S.; Kojima, K.; Sode, K. Review of Glucose Oxidases and Glucose Dehydrogenases: a Bird's Eye View of Glucose Sensing Enzymes. *J. Diab. Sci. Tech.* **2011**, 5, 1068-1076.
14. Tsujimura, S.; Kojima, S.; Kano, K.; Ikeda, T.; Sato, M.; Sanada, H.; Omura, H. Novel FAD-dependent Glucose Dehydrogenase for a Dioxygen-insensitive Glucose Biosensor. *Bios. Biot. Biochem.* **2006**, 70, 654-659.
15. Zakeeruddin, S. M.; Fraser, D. M.; Nazeeruddin, M. K.; Grätzel, M. Towards Mediator Design: Characterization of Tris-(4,4′-substituted-2, 2′-bipyridine) Complexes of Iron (II), Ruthenium (II) and Osmium (II) as Mediators for Glucose Oxidase of Aspergillus Niger and Other Redox Proteins. *J. Electroanal. Chem.* **1992**, 337, 253-283.
16. Nazeeruddin, M. K.; Zakeeruddin, S. M.; Kalyanasundaram, K. Enhanced Intensities of the Ligand-to-metal Charge-transfer Transitions in Ruthenium (III) and Osmium (III) Complexes of Substituted Bipyridines. *J. Phys. Chem.* **1993**, 97, 9607-9612.
17. Kim, H. H.; Mano, N.; Zhang, Y.; Heller, A. A Miniature Membrane-less Biofuel Cell Operating Under Physiological Conditions at 0.5 V. *J. Electrochem. Soc.* **2003**, 150, A209.
18. Jeon, W. Y.; Lee, C. J.; Choi, Y. B.; Lee, B. H.; Jo, H. J.; Jeon, S. Y. Kim, H. H. Glucose Detection *via* Ru-mediated Catalytic Reaction of Glucose Dehydrogenase. *Adv. Mat. Let.* **2018**, 9, 220-224.
19. Gregg, B. A.; Heller, A. Cross-linked Redox Gels Containing Glucose Oxidase for Amperometric Biosensor Applications. *Anal. Chem.* **1990**, 62, 258-263.
20. Qiu, J. D.; Zhou, W. M.; Guo, J.; Wang, R.; Liang, R. P. Amperometric Sensor Based on Ferrocene-modified Multiwalled Carbon Nanotube Nanocomposites as Electron Mediator for the Determination of Glucose. *Anal. Biochem.* **2009**, 385, 264-269.
21. Kalyanasundaram, K.; Zakeeruddin, S. M.; Nazeeruddin, M. K. Ligand to Metal Charge Transfer Transitions in Ru (III) and Os (III) Complexes of Substituted 2,2′-bipyridines. *Coord. Chem. Rev.* **1994**, 132, 259-264.
22. Forster, R. J.; Vos, J. G. Synthesis, Characterization, and Properties of a Series of Osmium-and Ruthenium-containing Metallopolymers. *Macromolecules* **1990**, 23, 4372-4377.
23. Fodor, C.; Bozi, J.; Blazsó, M.; Ivan, B. Thermal Behavior, Stability, and Decomposition Mechanism of Poly(*N*-vinylimidazole). *Macromolecules* **2012**, 45, 8953-8960.
24. Geraty, S. M.; Vos, J. G. Synthesis, Characterisation, and Photochemical Properties of a Series of Ruthenium Containing Metallopolymers Based on Poly-*N*-vinylimidazole. *J. Chem. Soc. Dalt. Trans.* **1987**, 3073-3078.
25. van der Westhuizen, D.; von Eschwege, K. G.; Conradie, J. Electrochemistry and Spectroscopy of Substituted [Ru (phen) 3] 2+ and [Ru (bpy) 3] 2+ Complexes. *Electro. Act.* **2019**, 320, 134540.
26. Kavanagh, P.; Leech, D. Improved Synthesis of 4,4′-diamino-2, 2′-bipyridine from 4,4′-dinitro-2, 2′-bipyridine-*N*,*N*′-dioxide. *Tetra. Let.* **2004**, 45, 121-123.
27. Guo, D.; Zhuo, Y. Z.; Lai, A. N.; Zhang, Q. G.; Zhu, A. M.; Liu, Q. L. Interpenetrating Anion Exchange Membranes Using Poly (1-vinylimidazole) as Bifunctional Crosslinker for Fuel Cells. *J. Mem. Sci.* **2016**, 518, 295-304.
28. Zhao, W.; Tang, Y.; Xi, J.; Kong, J. Functionalized Graphene Sheets with Poly(ionic liquid) s and High Adsorption Capacity of Anionic Dyes. *App. Sur. Sci.* **2015**, 326, 276-284.
29. Talu, M.; Demiroğlu, E. U.; Yurdakul, Ş.; Badoğlu, S. FTIR, Raman and NMR Spectroscopic and DFT Theoretical Studies on Poly(*N*-vinylimidazole). *Spect. Act. Part A: Mole. Bio. Spec.* **2015**, 134, 267-275.
30. Edmiston, M. J. *An Evaluation of Surface-Enhanced Raman Spectroscopy (SERS) as a Chemical Sensing Technique*. University of Glasgow (United Kingdom), **1991**.
31. Athanas, A. B.; Subramaniam, K.; Thangaraj, S.; Kalaiyar, S. Amine Functionalized Homoleptic Ruthenium (II) Sensitizer for Dye-sensitized Solar Cells: a Combined Effect of Ancillary Ligands and Co-sensitization. *Int. J. En. Res*. **2020**, 44, 1899-1908.
32. Nazeeruddin, M. K.; Zakeeruddin, S. M.; Kalyanasundaram, K. Enhanced Intensities of the Ligand-to-metal Charge-transfer Transitions in Ruthenium (III) and Osmium (III) Complexes of Substituted Bipyridines. *J. Phys. Chem.* **1993**, 97, 9607-9612.
33. Pekel, N.; Savaş, H.; Güven, O. Complex Formation and Adsorption of V 3+, Cr 3+ and Fe 3+ ions with Poly(*N*-vinylimidazole). *Col. Poly. Sci.* **2002**, 280, 46-51.
34. Guo, J.; Yu, P.; Wang, H.; Zhao, H. Design and Synthesis of 4, 4′-disubstituted-[2,2′]-bipyridines for Catalyzing CO/styrene Copolymerization with Palladium (II). *Trans. Tian. Univ.* **2015**, 21, 406-411.
35. Lippert, J. L.; Robertson, J. A.; Havens, J. R.; Tan, J. S. Structural

Studies of Poly(*N*-vinylimidazole) Complexes by Infrared and Raman Spectroscopy. *Macromolecules* **1985**, 18, 63-67.
36. Küçükyavuz, Z.; Küçükyavuz, S.; Abbasnejad, N. Electrically Conductive Polymers from Poly(*N*-vinylimidazole). *Poly.* **1996**, 37, 3215-3218.
37. Freitas, C.; Müller, R. H. Effect of Light and Temperature on Zeta Potential and Physical Stability in Solid Lipid Nanoparticle (SLN^{TM}) Dispersions. *Int. Pharm*. **1998**, 168, 221-229.
38. Kissinger, P. T.; Heineman, W. R. Cyclic Voltammetry. *J. Chem. Edu.* **1983**, 60, 702.
39. Leftheriotis, G.; Papaefthimiou, S.; Yianoulis, P. Dependence of the Estimated Diffusion Coefficient of LixWO_3 Films on the Scan Rate of Cyclic Voltammetry Experiments. *Sol. S. Ion.* **2007**, 178, 259-263.
40. Hagel, A. F.; Albrecht, H.; Dauth, W.; Hagel, W.; Vitali, F.; Ganzleben, I.; Schultis, H. W.; Konturek, P. C.; Stein, J.; Neurath, M. F.; Raithel, M. Plasma Concentrations of Ascorbic Acid in a Cross Section of the German Population. *J. Int. Med. Res.* **2018**, 46, 168-174.
41. Hsine, Z.; Blili, S.; Milka, R.; Dorizon, H.; Said, A. H.; Korri-Youssoufi, H. Sensor Based on Redox Conjugated Poly(para-phenylene) for the Simultaneous Detection of Dopamine, Ascorbic Acid, and Uric Acid in Human Serum Sample. *Anal. Bioanal. Chem.* **2020**, 412, 4433-4446.
42. Lakshmi, D.; Whitcombe, M. J.; Davis, F.; Sharma, P. S.; Prasad, B. B. Electrochemical Detection of Uric Acid in Mixed and Clinical Samples: a Review. *Electroanal.* **2011**, 23, 305-320.